

# Novolac Epoxy Resins and Positron Annihilation

T. SUZUKI,<sup>1,\*</sup> Y. OKI,<sup>1</sup> M. NUMAJIRI,<sup>1</sup> T. MIURA,<sup>1</sup> K. KONDO,<sup>1</sup> Y. SHIOMI,<sup>2</sup> and Y. ITO<sup>3</sup>

<sup>1</sup>National Laboratory for High Energy Physics, Radiation Control Center, Oho, Tsukuba, Ibaraki, 305, Japan; <sup>2</sup>Tsukuba Research Laboratory, Sumitomo Chemical Co. Ltd., Kitahara, Tsukuba, Ibaraki, 300-32, Japan; and <sup>3</sup>Research Center for Nuclear Science and Technology, The University of Tokyo, Tokaimura, 319-11, Japan

## SYNOPSIS

Four kinds of epoxy resins: cresol novolac, tris-hydroxyphenylmethane, tetramethylbiphenol, and bisphenol A, were cured with phenol novolac epoxy resins. Characteristics of these epoxy compounds were studied by the positron annihilation lifetime (PAL) technique. Glass transition temperatures, thermal expansion coefficients, and volume of intermolecular-space holes among polymer chains were obtained from the lifetime,  $\tau_3$ , of the long-lived component of *ortho*-positronium. It was revealed that, at the glass transition temperature,  $T_g$ , the volume of the hole created among polymer chains expanded 1.4 times the volume at room temperature. The smaller flexural modulus of tris-hydroxyphenylmethane than that of the other samples was explained by the volume of intermolecular-space holes obtained from  $\tau_3$ . Aging effects were seen in the data of the intensities,  $I_3$ , of *ortho*-positronium, which became smaller after heating the samples above  $T_g$ .  $I_3$  and  $\tau_3$  were strongly affected by the density of cross-linkings and their chemical structures. The larger the density of cross-linkings, the smaller  $I_3$  and higher  $T_g$  were obtained. Epoxy compounds with the higher water-absorption rates had larger intermolecular-space holes. © 1993 John Wiley & Sons, Inc.

## 1. INTRODUCTION

Epoxy resins have been extensively employed as encapsulating materials of integrated circuits (ICs) to protect semiconductor chips and circuits from moisture, dusts, shocks, and other external obstructions as well as to secure the electrical insulation. Hence, the development and the reliability of ICs and large scale ICs (LSI) depend on the improvement of the encapsulating technique and its materials.<sup>1</sup>

Among many types of epoxy resins, novolac epoxy resins are widely used for the encapsulation.<sup>2</sup> Since they have many epoxy groups to develop cross-linkings, they have high mechanical strength and high glass transition temperatures. Commonly, cresol novolac epoxy resins are cured with phenol novolac epoxy resins and the product has high moisture resistance, high heat resistance, and good moldability. There have been many efforts to develop better en-

capsulating materials from various combinations of novolac epoxy resins and other hardeners.<sup>3,4</sup>

There are many methods to test the characteristics of new materials. Standard methods such as mechanical, electrical, chemical, and thermomechanical tests give macroscopic characteristics. To determine the microscopic structure of polymers, positron annihilation (PA) has been applied in the last decade<sup>5</sup> to examine the intermolecular-space characteristics. This analysis utilizes the unique characteristics of PA, and polymer structures of the order of nanometers (nm) can be studied. Especially, the volume of intermolecular-space holes can be quantitatively determined. There are many models to estimate the excess volume fraction in polymers.<sup>6</sup> However, in most cases, the fraction can be obtained indirectly. From this point of view, PA is expected to give an alternative novel technique to estimate the excess volume fraction. The details of PA are given elsewhere.<sup>7,8</sup>

Positrons emitted from radioisotopes (e.g., <sup>22</sup>Na) with an energy of a few hundred keV lose their energy through inelastic atomic collisions. Finally, they are annihilated with electrons via several processes,

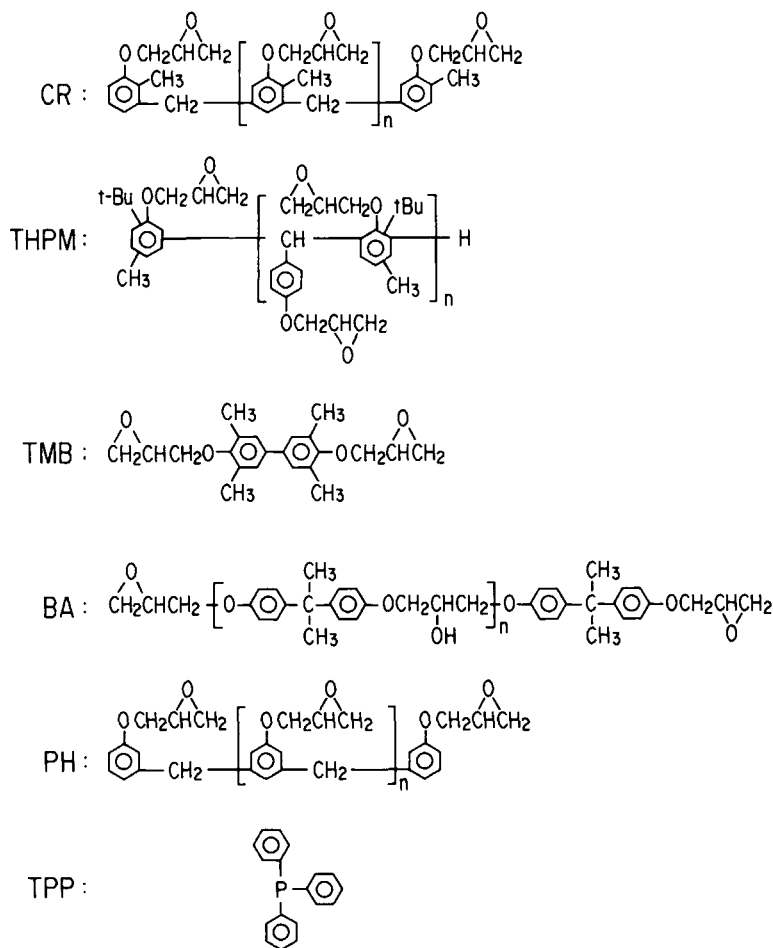
\* To whom correspondence should be addressed.

emitting 511 keV gamma rays. Especially, positrons in a polymer form a bound state with an electron called a positronium (Ps). There are two types of Ps depending on the spin direction: *para*-Ps (*p*-Ps) and *ortho*-Ps (*o*-Ps), which have lifetimes of 0.125 and 140 ns *in vacuo*, respectively. Ps seeks intermolecular-space holes and can remain inside the hole until it picks up an electron: the so-called pick-off annihilation. The lifetime and the intensity of *o*-Ps depend on the volume and the number, respectively, of intermolecular-space holes. The intermolecular-space holes in polymers are affected strongly by the states (liquid or solid), temperature, defects, crystallinity, and so on. Hence, PA has been applied to study phase or state transition.<sup>9,10</sup> Furthermore, Okamoto et al.<sup>11</sup> reported that Ps formation is also chemically affected by the function groups of polymers.

In this work, four kinds of epoxy resins were cured with phenol novolac epoxy resins. Characteristics of these epoxy resins were measured by several standard methods. The glass transition temperatures, linear expansion coefficients, mechanical strengths, and moisture absorption rates were obtained. Also, positron annihilation lifetime (PAL) measurements were applied to study the characteristics of these samples from the point of view of nanometer holes. The results obtained by the standard methods will be compared with those of the PAL measurements.

## 2. EXPERIMENTAL

The positron annihilation (PA) experiments were conducted with a conventional fast-fast coincidence system with a time resolution of 0.27 ns full-width



at half-maximum (fwhm). The details of the experimental setup are given elsewhere.<sup>8,12</sup> Two positron sources were prepared by depositing about 30  $\mu\text{Ci}$  of aqueous  $^{22}\text{NaCl}$  on a thin nickel foil of 2.8  $\text{mg}/\text{cm}^2$  thickness and area of  $5 \times 5$  mm, which was then covered with another foil of the same size. The sources were sealed with 3  $\mu\text{m}$  Mylar films and, then, sandwiched by two identical samples ( $10 \times 20 \times 2$  mm) for PAL measurements.

Four kinds of epoxy resins—cresol novolac (CR), tris-hydroxyphenylmethane (THPM), tetramethylbiphenol (TMB), and bisphenol-A (BA)—were cured with a hardener—phenol novolac epoxy resins (PH)—to prepare four kinds of epoxy compounds, adding triphenylphosphin as a catalyst. The molecular structures are presented in Figure 1. The mix-

tures of the resin and the hardener were heated at 175°C and pressed and molded for 5 min, then cured at 180°C for 5 h and finally cooled down to room temperature in 4 h. The mixing ratio of resin, hardener, and catalyst in weight is presented in Table I.

The temperature of the samples was increased from the lowest temperature around 30°C up to the highest temperature around 200°C at the rate of 5°C/h. When the temperature reached the highest point, it was maintained for 1 h and then was decreased to the lowest temperature at the same rate. As shown in Figures 3–5, different temperature ranges were employed for each sample according to the different glass transition temperatures. PAL spectra were obtained at every hour, i.e., at every

**Table I** Characteristics of Epoxy Compounds

	Sample No.			
	1 (CR)	2 (THPM)	3 (TMB)	4 (BA)
Epoxy resin (mixing ratio) <sup>a</sup>	Cresole novolac (100)	Tris-hydroxyphenylmethane (100)	Tetramethylbiphenol (100)	Bisphenol A (100)
Hardener:				
Phenol novolac (mixing ratio) <sup>a</sup>	(56.4)	(51.6)	(56.7)	(61.8)
Catalyst:				
Triphenylphosphin (mixing ratio) <sup>a</sup>	(1.5)	(1.5)	(1.5)	(1.5)
Density ( $\text{g}/\text{cm}^3$ )	1.22	1.14	1.20	1.21
Flexural modulus ( $\text{kg}/\text{mm}^2$ )	342	279	309	290
Water absorption <sup>b</sup>				
98°C 1 h (%)	0.47	0.88	0.46	0.45
Saturation (%)	2.44	2.46	2.26	2.34
PA at 98°C				
Volume ( $\text{nm}^3$ )	0.095	0.120	0.098	0.97
Intensity $I_3$ (%)	23.0	22.0	27.5	26.2
$T_g$ (°C) by TMA	192	204	139	140
$T_g$ (°C) by PA	163	185	132	130
Volume ( $\text{nm}^3$ )	0.110	0.136	0.110	0.104
Linear expansion coefficient $1/^\circ\text{C}$				
$\alpha'$ by TMA ( $< T_g$ )	6.5E-5	7.5E-5	5.3E-5	6.3E-5
$\alpha''$ by PA ( $< T_g$ )	9 E-4	6 E-4	12 E-4	29 E-4
( $\sim T_g$ )	16 E-4	15 E-4	23 E-4	63 E-4

Abbreviations are as follows:  $T_g$ , glass transition temperature; TMA, thermomechanical analysis; PA; positron annihilation.

<sup>a</sup> The mixing ratios are shown in weight.

<sup>b</sup> Water-absorption rate was measured by immersing samples in water controlled at 98°C.

5°C. The temperature was measured with a copper/nickel T thermocouple, which was placed between two samples. The heat cell separated the two plastic scintillation counters 2.6 cm apart, and two million events were collected in one PAL spectrum. The lifetime spectra were analyzed by the program POSITRONFIT EXTENDED<sup>13</sup> and were resolved into three lifetime components.

### 3. RESULTS AND DISCUSSION

#### 3.1. Intensities and Lifetimes of Positron Annihilation Spectra

In polymers, positrons form Ps, and a typical lifetime spectrum is shown in Figure 2. Generally, the annihilation spectra of polymers can be deconvoluted into three or four components. In polyethylenes,<sup>14,15</sup> Teflons,<sup>16</sup> and polypropylenes,<sup>17</sup> the spectra have been deconvoluted into four components. In these samples, two long-lived components attributable to *o*-Ps are always resolvable. However, the PAL spectra of the epoxy compounds could not be deconvoluted into four components. Hence, in this work, all spectra have been analyzed with three components. The first component has a lifetime  $\tau_1$  around 0.20–0.25 ns, to which *p*-Ps and other short lifetime components contribute. The second component has a lifetime  $\tau_2$  around 0.5 ns attributable to positrons that do not form Ps. A long-lived component (*o*-Ps) lifetime  $\tau_3$  ranges from 1.8 to 2.6 ns. In the analysis, the fitting errors of intensities of the first ( $I_1$ ) and the second ( $I_2$ ) components were around 8%, whereas those of the third component was around 1%. Also, the fitting errors of  $\tau_1$  and  $\tau_2$  were five

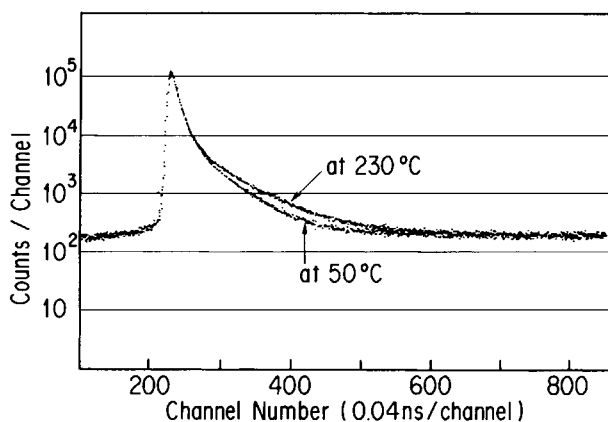


**Figure 2** Typical PA lifetime spectra taken at 50 and 230°C for epoxy compounds of CR cured with PH. Abbreviations are presented in the legend of Figure 1.

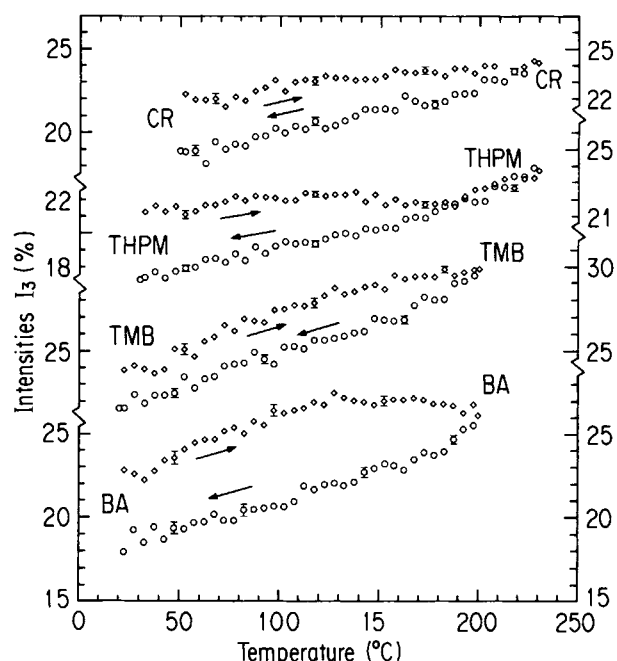


**Figure 3** Intensities  $I_3$  of long-lived component for ( $\diamond$ ) heating and ( $\circ$ ) cooling processes vs. temperature. Abbreviations are presented in the legend of Figure 1.

times larger than those of  $\tau_3$ , which was about 0.6%. Hence, the intensity and the lifetime of the long-lived component are derived with high accuracy.

The results of  $I_3$  [( $\diamond$ ) heating process; ( $\circ$ ) cooling process] are shown in Figure 3 for the four samples, which presents physical aging. Figures 4 and 5 arrange  $I_3$  presented in Figure 3 in heating and cooling processes, respectively. Thus, it helps to compare variations of four samples in each process. Since, as shown in Figure 6, the variations of  $\tau_3$  in the both processes are almost the same,  $\tau_3$  and its volume of the heating process are presented in Figure 7.

#### 3.2. Intensities of the Long-lived Components

$I_3$  of the four samples in the cooling process were smaller than that in the heating process (Fig. 3), which can be attributed to a physical aging effect. In preparing epoxy compounds, the samples were pressed at 175°C for 5 min, and during this process, defects and strains might be introduced due to possible incomplete curing, resulting in an increased number of intermolecular-space holes. After heating the samples above  $T_g$ , most of the defects and the strains must have been annealed out and this was reflected in the decrease in the  $I_3$  value. Epoxies that undergo physical aging change in mechanical properties<sup>18</sup> and in physical properties.<sup>19</sup> It was ob-

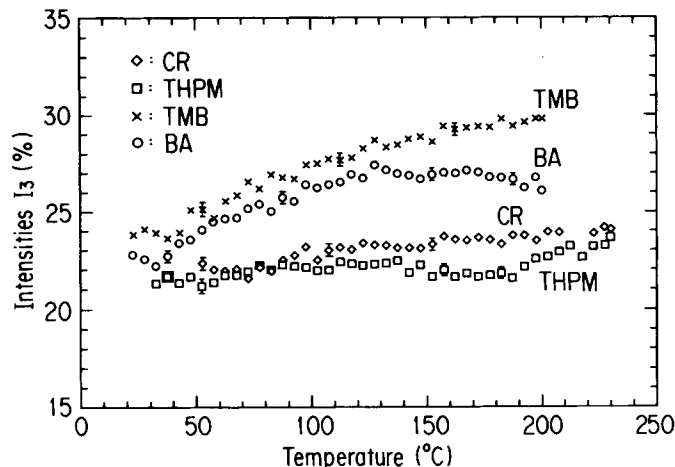


**Figure 4** Intensities  $I_3$  of long-lived component for heating process vs. temperature. Abbreviations are presented in the legend of Figure 1.

served that a high density was obtained in highly aged epoxies,<sup>19</sup> which is consistent with the decrease of  $I_3$ .

Figures 3 and 4 show that variation of  $I_3$  in the heating process is quite smaller than that in the cooling process. In the case of CR and THPM, the increases of  $I_3$  below the glass transition  $T_g$  ( $\sim 200^\circ\text{C}$ ) were about 2 and 1%, respectively, which were smaller than the 4% of TMB and BA. This can be explained by chemical structures, from which the density of cross-linkings is expected to be larger in epoxy compounds of CR and THPM than that of TMB and BA. The small changes of  $I_3$  imply that the polymer structure is not affected much with increasing temperature and the number of intermolecular-space holes in samples are quite constant even at higher temperatures. Considering the chem-

ical structures, quite rigid structures of three-dimensional networks are expected to develop in CR and THPM, and intermolecular-space holes are formed among these networks. Perhaps, even if the temperatures of CR and THPM samples are increased, the rigid structures containing the holes and strains may not change much to produce additional intermolecular-space holes. After annealing at temperatures above  $T_g$ , the variation of the cooling process is different from that of the heating process, and as seen in Figure 5,  $I_3$  of the four samples decreases with decreasing temperature.

In Figure 4, the  $I_3$ 's of TMB and BA are larger than those of CR and THPM for the whole temperature range, which is also attributed to the density of cross-linkings. Comparing TMB with BA, TMB has much simpler chemical structures, re-

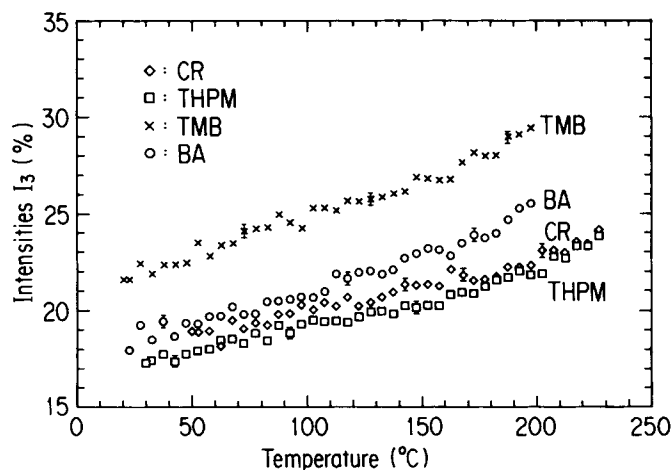


**Figure 5** Intensities  $I_3$  of long-lived component for cooling processes vs. temperature. Abbreviations are presented in the legend of Figure 1.

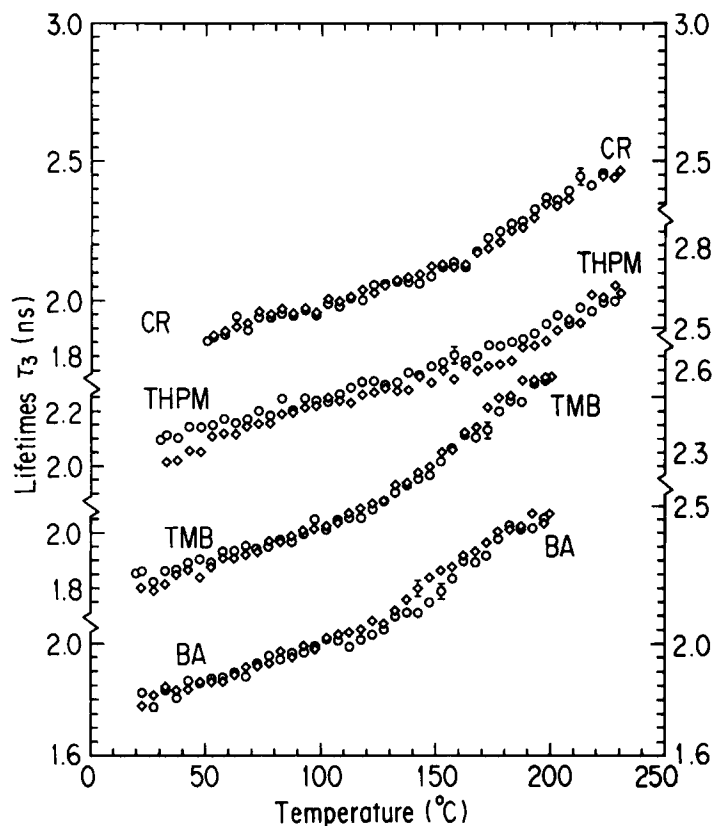


**Figure 6** Lifetimes  $\tau_3$  of long-lived component for ( $\diamond$ ) heating and ( $\circ$ ) cooling processes. Abbreviations are presented in the legend of Figure 1.

sulting in the large  $I_3$  of TMB. In the cooling process (Fig. 5),  $I_3$  of TMB is quite larger than that of the other three samples for the whole temperature region. This may be the result of the physical aging effect as seen in Figure 3, and the differences in  $I_3$

before and after annealing are 2% for TMB and 4% for the other three samples at room temperature. This suggests that defects and strains in TMB introduced during the premolding process were less than those in the other samples.

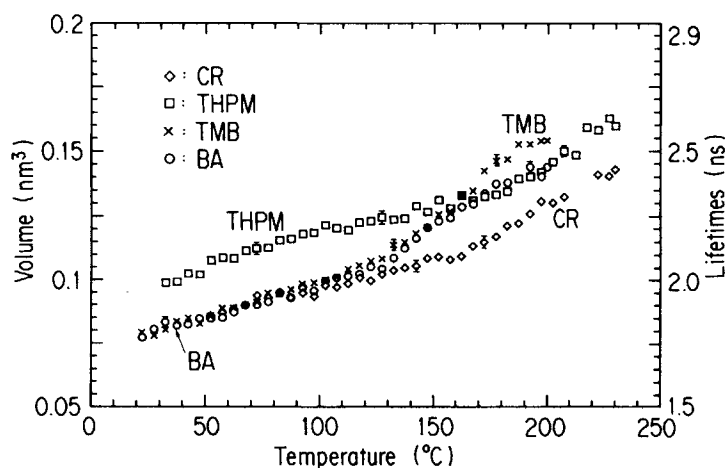


**Figure 7** Lifetimes  $\tau_3$  of long-lived component for heating process. Abbreviations are presented in the legend of Figure 1.

### 3.3. Lifetimes and Volume of Intermolecular-space Holes

$\tau_3$  is correlated with the volume of intermolecular-space holes in which Ps is trapped. The relation is described as<sup>9,20,21</sup>

$$\tau_3 = 0.5 \times [1 \times R/(R + \Delta R) + 1/(2\pi) \times \sin\{2\pi \times R/(R + \Delta R)\}]^{-1} \quad (1)$$

where the intermolecular-space holes are assumed to be a sphere with a radius of  $R$  and an electron layer of thickness  $\Delta R = 0.166$  nm. Using this equation, the hole volume corresponding to  $\tau_3$  for the heating process was calculated and the results are shown in Figure 7 together with the lifetime. Figure 7 shows results as follows: (1)  $\tau_3$  (or hole volume) of CR, TMB, and BA change in a similar way up to around 130°C, which is close to the  $T_g$  for TMB and BA determined by PAL (Table I); (2)  $\tau_3$  (or hole volume) of THPM is larger than those of the other samples below 150°C. The large  $\tau_3$  of THPM can be expected from their chemical structures. Since THPM has extending side chains in the opposite directions (Fig. 1), intermolecular spaces among cross-linkings should be larger in THPM than those in the other samples. At room temperature, the volume of intermolecular-space holes determined by  $\tau_3$  was almost 0.1 nm<sup>3</sup> for THPM and 0.075 nm<sup>3</sup> for CR, TMB, and BA.

### 3.4. Glass Transition Temperature and Thermal Expansion Coefficient

From the variation of volume with increasing temperature, volume and/or linear expansion coefficients and  $T_g$  can be obtained. Below  $T_g$ , the expansion coefficient for the glass state is obtained, and above  $T_g$ , that for the rubbery state. The results calculated from Figure 7 are presented in Table I together with the results determined by thermo-mechanical analysis (TMA). It suggests that  $T'_g$  determined by TMA is larger than  $T''_g$  by PA (henceforth, the values determined by TMA and PA will be shown with ' and ', respectively). The difference  $\Delta T_g (= T'_g - T''_g)$  was larger for CR and THPM than for TMB and BA:  $\Delta T_g = 29^\circ\text{C}$  for CR,  $19^\circ\text{C}$  for THPM,  $7^\circ\text{C}$  for TMB, and  $10^\circ\text{C}$  for BA. It is quite probable that  $T''_g$  is lower than  $T'_g$ , because  $T''_g$  is related to the onset of the micro-Brownian motions of small regions of molecular structures, whereas  $T'_g$  is related to the movement of the large scale of the polymer structures. Since the regions around

the intermolecular-space hole, in which Ps is trapped, are distorted due to defects or strains, the segments are considered to become movable even below  $T'_g$ , resulting in lower  $T''_g$ .

The results of  $\Delta T_g$  listed above show that they are larger for epoxy compounds with high cross-linking densities (CR and THPM) than for those with low cross-linking densities (TMB and BA). Also, it can be expected that  $T'_g$  is higher for the former samples than for the latter samples (Table I). This is also observed for  $T''_g$ , even though  $T''_g$  occurs at quite lower temperatures than does  $T'_g$ . From the chemical structures of CR and THPM, the cross-linking densities of THPM are expected to be higher than those of CR. Thus, it seems that the result of higher  $T'_g$  and  $T''_g$  of THPM than those of CR is related to the cross-linking densities.

As shown in Figure 7, intermolecular-space holes created in THPM are larger than those in CR and this reduces the flexural modulus of THPM, since one of the factors to determine the flexural modulus is the volume of holes created among polymer structures.<sup>22</sup> Thus, the quantitative determination of hole volume among polymer chains by PAL is useful to study modulus of polymers.

$T_g$  is defined as follows<sup>23</sup>: At  $T_g$ , the intermolecular free space of molecules becomes so small that molecular movements of the whole molecule or of large-chain segments are no longer possible. It is noteworthy that the  $T''_g$  of CR, TMB, and BA occurred when the volume of intermolecular-space holes attained the volume of  $\sim 0.11$  nm<sup>3</sup>. For these samples, the ratios of volumes at  $T_g$  to those at room temperature are about 1.4. In the case of CR, the volume of  $T_g$  is 0.136 nm<sup>3</sup>, being larger than that of the other samples, but the ratio is almost the same value of 1.4. These results suggest that, when polymers become rubbery, the volume of intermolecular-space holes expanded to a certain volume with increasing temperature. From this point of view, the difference of  $T'_g$  and  $T''_g$  can be explained by the volume of the space;  $T'_g$  relates the movement of large polymer chains and segments required for the expansion of bulk and  $T''_g$  is obtained from the expansion of intermolecular-space holes, which requires the movement of a small part of the polymer chains surrounding the hole. Thus,  $T'_g$  is expected to be higher than  $T''_g$ .

The linear expansion coefficients  $\alpha''$  are almost 10 times larger than  $\alpha'$  (Table I). This can be explained by the fact that  $\alpha'$  is related to the expansion of bulk, and  $\alpha''$ , to the expansion of intermolecular-space holes. As discussed above for  $T_g$ , the small segments of polymer chains around the holes can

move easily with increasing temperature. From the results of PA,  $\alpha''$  of CR and THPM are smaller than those of TMB and BA, which can be expected from the density of cross-linkings.

### 3.5. Water-Absorption Rate and Polymer Structures

In Table I, the data of water absorption in four samples are presented. For these measurements, the samples were immersed in a water bath controlled at about 98°C, slightly below the boiling temperature. Three samples, CR, TMB, and BA, showed almost similar absorption rates, whereas THPM absorbed water twice as fast as did the others. Since THPM has a larger  $\tau_3$  value (hence, larger intermolecular-space holes) than that of the other samples (Table I), the correlation between  $\tau_3$  and the absorption rate seems evident. This agrees with the well-known relation between the self-diffusion coefficient  $D$  and the free-volume fraction  $V_f$ <sup>24</sup>:

$$D = A \times \exp(-B/V_f)$$

where  $A$  and  $B$  are constants. The diffusion of solutions into polymers have been reported for many types of solutions. According to results of the diffusion coefficient of moisture into epoxy resin compounds<sup>25</sup> and polyimides,<sup>26</sup> it was shown that the diffusion coefficient was larger for polymers with a larger fraction of intermolecular space, as expected from the free-volume theory.

The product of PA parameters  $F = I_3 \times V_h$ , where  $V_h$  is the volume of intermolecular-space holes estimated from  $\tau_3$ , is often considered to be the measure of the fraction of intermolecular space.  $F$  is calculated from Table I to be 0.022 for CR, 0.026 for THPM, 0.027 for TMB, and 0.025 for BA.

Since  $I_3$  is affected strongly by chemical structures such as electron affinity<sup>11</sup> (e.g., few Ps is formed in Kapton, one of polyimide compounds), it is not simple to compare  $I_3$  of polymers with different chemical structures. In our case, THPM and CR have similar chemical structures and it can be pointed out that the water-absorption rate of THPM is larger than that of CR (Table I), as expected from  $F$  shown above. Also, for the case of TMB and BA with similar chemical structures, the absorption rates are almost the same, being consistent with the results of similar  $F$  shown above. Although  $F$  of TMB and BA are almost equal to  $F$  of THPM, former absorption rates are smaller than those of the latter one, which shows that  $F$  is not consistent

with the absorption rates of polymers with different chemical structures.

## 4. CONCLUSION

Positron annihilation has been applied to study novolac epoxy resins and has been proven to be a useful analytical method to investigate characteristics of polymers.

Generally, in preparing epoxy compounds, defects and strains are introduced. From PA, the physical aging effect was observed in the difference of  $I_3$  between heating and cooling processes and it was small in TMB compared with CR, THPM, and BA. Rigid structures expected from the density of cross-linkings for THPM and CR were reflected in  $I_3$ , which was constant for the whole temperature range in the heating process. It was observed that  $I_3$  of THPM and CR with a higher density of cross-linkings was larger than  $I_3$  of BA and TMB.

$\tau_3$  is correlated with the volume of intermolecular-space holes. From the variation of volume determined by  $\tau_3$  with increasing temperature, glass transition temperatures ( $T_g$ ) and thermal (volume and/or linear) expansion coefficient ( $\alpha$ ) can be obtained, which concerns the movement of molecular microstructures and are different from those determined by TMA. The difference between  $T_g$  determined by TMA and PA,  $\Delta T_g$ , is larger in THPM and CR than that in BA and TMB, which may be attributed to the density of cross-linkings. It has been observed that the higher the cross-linking density is the larger the  $\Delta T_g$  obtained. For CR and THPM,  $\alpha$  determined by PA is 10 times larger than that by TMA, whereas for TMB and BA, it is 20–50 times larger than that by TMA. The results suggest that the density of cross-linking strongly affects the movement of chains.

For the four samples, the volume determined by  $\tau_3$  at  $T_g$  was found to be 1.4 times larger than those at room temperature. It is considered that enough space is needed for the small segment of polymer chains to become movable at the glass transition temperature and the expansion of space becomes 1.4 times that of volume at room temperature for these epoxy compounds.

Epoxy compounds consisting of THPM have a low moisture resistance compared with other novolac epoxy compounds and this is consistent with the fact that the hole volume determined by  $\tau_3$  is larger than those of the others. This also is consistent with the small flexural modulus of THPM.



This work is supported in part by the Grant-in-Aid of the Japanese Ministry of Education, Culture and Science.

## REFERENCES

1. K. Iko, Y. Nakamura, M. Yamaguchi, and N. Imamura, *IEEE Elect. Insulat. Mag.*, **6**, 25–32 (1990).
2. M. Shinpo, *Handbook of Epoxy Resins* (in Japanese) M. Shinpo, Ed., Nikkann Kougyou, Tokyo, 1987.
3. S. Kanagawa and Y. Terada, *Mater. Res. Soc. Proceed.*, **72**, 205–216 (1986).
4. M. Ogata, N. Kinjo, S. Eguchi, H. Hozoji, T. Kawata, and H. Sasima, *J. Appl. Polym. Sci.*, **44**, 1795–1805 (1992).
5. Y. C. Jean, *Microchem. J.*, **42**, 72–102 (1990).
6. V. B. Gupta and C. Brahatheeswaran, *Polymer*, **32**, 1875–1884 (1991).
7. Y. Ito, H. Kaji, Y. Tabata, and K. Yoshihara, *Soryusi no Kagaku* (in Japanese) (*Chemistry of Elementary Particles*), Gakkai Shuppan Center, Tokyo, 1985.
8. D. M. Schrader and Y. C. Jean, *Positron and Positronium Chemistry*, Elsevier, Amsterdam, 1988.
9. M. Eldrup, D. Lightbody, and J. N. Sherwood, *Chem. Phys.*, **63**, 51–58 (1981).
10. D. Lightbody, J. N. Sherwood, and M. Eldrup, *Chem. Phys.*, **93**, 475–484 (1985).
11. K. Okamoto, K. Tanaka, M. Katsube, O. Sueoka, and Y. Ito, to appear.
12. T. Suzuki, Y. Ito, K. Endo, S. Fujita, Y. Masuda, and T. Egusa, *Int. J. Appl. Radiat. Isot.*, **39**, 53–57 (1988).
13. P. Kirkegaard and M. Eldrup, *Comput. Phys. Commun.*, **7**, 401–409 (1974).
14. P. Kindl and G. Reiter, *Phys. Stat. Sol. (a)*, **104**, 707–713 (1987).
15. T. Suzuki, Y. Oki, M. Numajiri, T. Miura, T. Kondo, and Y. Ito, *J. Polym. Sci. Polym. Phys.* **30**, 517–525 (1992).
16. P. Kindl and H. Sorman, *Phys. Stat. Sol. (a)*, **66**, 627–633 (1981).
17. A. Uedono, Y. Ohko, S. Watauchi, and Y. Ujihira, in *International Symposium on Material Chemistry in Nuclear Environment*, Tsukuba, Japan, March 12–13, 1992.
18. G. B. McKenna, M. M. Santore, A. Lee, and R. S. Duran, *J. Non-Cryst. Solids*, **131–133**, 497–504 (1991); A. Lee and G. B. McKenna, *Polym. Eng. Sci.*, **30**, 431–435 (1990).
19. I.-C. Choy and D. J. Plazek, *J. Polym. Sci. Part B*, **24**, 1303–1320 (1986).
20. H. Nakanishi and Y. C. Jean, in *Positron and Positronium Chemistry*, Elsevier, Amsterdam, 1988, pp. 159–192.
21. S. J. Tao, *J. Chem. Phys.*, **56**, 5499–5510 (1972).
22. A. Garton, P. D. McLean, W. T. K. Stevenson, J. N. Clark, and J. H. Daly, *Polym. Eng. Sci.*, **27**, 1620–1626 (1987).
23. D. W. Van Kevelen, *Properties of Polymers: Their Estimation and Correlation with Chemical Structure*, Elsevier, Amsterdam, Oxford, New York, 1976.
24. M. H. Cohen and D. Turnbull, *J. Chem. Phys.*, **31**, 1164–1168 (1959).
25. V. B. Gupter, L. T. Drazal, and M. J. Rich, *J. Appl. Polym. Sci.*, **30**, 4467–4493 (1985).
26. K. Okamoto, N. Tanihara, H. Watanabe, K. Tanaka, H. Kita, A. Nakamura, Y. Kusuki, and K. Nakagawa, *J. Polym. Sci. Part B*, **30**, 1223–1231 (1992).

Received September 2, 1992

Accepted January 14, 1993